

## Impact of Non-Uniform Doping on the Plasmonic Properties of $\text{In}_2\text{O}_3$ Nanoparticles: A Study by Electron Energy Loss Spectroscopy

Sadegh Yazdi<sup>1</sup>, Ankit Agrawal<sup>2</sup>, Ajay Singh<sup>3</sup>, Delia J. Milliron<sup>2</sup> and Emilie Ringe<sup>1,4,5</sup>

- <sup>1</sup>. Department of Materials Science & Nano Engineering (MSNE), Rice University, Houston, USA.
- <sup>2</sup>. McKetta Department of Chemical Engineering, University of Texas at Austin, Austin, USA.
- <sup>3</sup>. Center for Integrated Nanotechnologies, Los Alamos National Laboratory, Los Alamos, USA.
- <sup>4</sup>. Department of Chemistry, Rice University, Houston, USA.
- <sup>5</sup>. Department of Materials Science and Metallurgy, University of Cambridge, Cambridge, United Kingdom.

Over the last two decades, research into light-matter interactions in metallic nanoparticles that support localized surface plasmon resonances (LSPRs) has enabled a vast range of applications from biomedicine to photocatalysis to optoelectronics [1]. In recent years, the range of materials used in plasmonic devices has been expanded beyond the conventional Ag and Au metallic nanostructures. Degenerately doped semiconductor nanoparticles (NPs) are one of the most promising materials for different plasmonic applications such as smart windows and sensing [2]. The unique advantage of semiconductor NPs over their metallic counterparts is that the carrier density in semiconductors can be tuned by dopant concentrations. By altering the dopant concentration in semiconductor NPs, the LSPR can be tuned to the desired frequency throughout the visible to mid-infrared range, as required by specific applications. However, the presence of surface states and defects on the surfaces of semiconductor NPs results in surface band bending and therefore the formation of surface depletion regions. The width of the depletion region depends on the dopant concentration; higher dopant concentrations leading to thinner depletion regions. The depletion width and carrier density close to the surface affect the plasmonic properties of semiconductor NPs. Here, we demonstrate the effect of dopant distribution on the evanescent plasmonic field decay length in F and Sn co-doped  $\text{In}_2\text{O}_3$  (FITO) nanocubes. We use monochromated electron energy loss spectroscopy (EELS) to map the LSPRs in individual FITO nanocubes with two different dopant distributions: nanocubes with higher dopant concentrations in the shell (shell-doped) and in the core (core-doped). Both core-doped and shell-doped FITO nanocubes that are studied here were synthesized using standard Schlenk line air-free colloidal synthesis techniques, as explained in [3].

Scanning transmission electron microscopy energy dispersive X-ray spectroscopy (STEM-EDS) mapping confirms the difference between the two nanocubes in terms of dopant distribution (Fig. 1 a and b). Atomic resolution high angle annular dark field STEM (HAADF-STEM) images show the high quality body-centred cubic bixbyite crystal structure of FITO nanocubes (Fig. 1 c). Analyzing monochromated STEM-EELS maps of 17 FITO nanocubes, 9 uniformly-doped and 8 surface-doped ones, revealed that the plasmonic field decay length changes significantly with the dopant distribution. To generate maps of the plasmon modes from STEM-EELS spectrum images, blind source separation via non-negative matrix factorization (NMF) was used [4]. Two LSPRs were obtained for all the cubes, one with high loss probability near the corners, the other, with high loss probability near the facets. In core-doped nanocubes, the decay length of the edge mode was larger than that of the corner mode, while the opposite was the case in the shell-doped FITO nanocubes (Fig. 2). This ability to chemically manipulate the extent of near-field in plasmonic structures holds promise for applications such as sensing and smart windows.

## References:

- [1] K. A. Willets and R. P. Van Duyne, *Annu. Rev. Phys. Chem.* **58** (2007) p. 267.  
 [2] O. Zandi *et al.* arXiv preprint arXiv:1709.07136 *Cond-Mat Physicsphysics* (2017) .  
 [3] A. Agrawal *et al.* *Nano letters* **17** (2017) p. 2611.  
 [4] S. Yazdi *et al.* *Nano letters* **16** (2016) p. 6939.

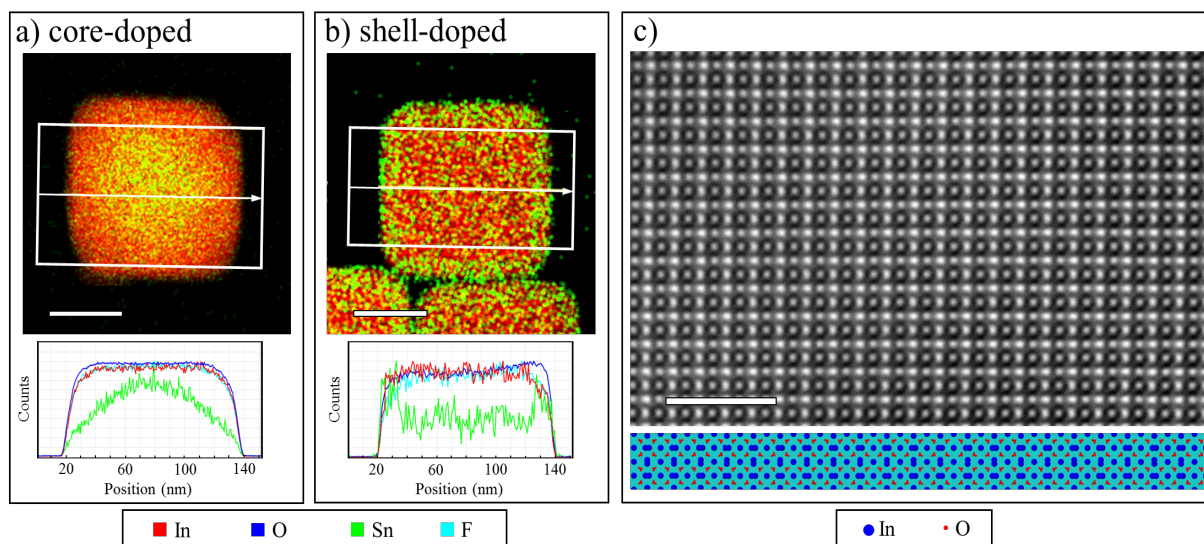


**Fig. 1)** STEM-EDS maps and their corresponding averaged line profiles of FITO nanocubes with Sn dopant concentrations higher in the a) core (core-doped) and b) shell (shell-doped). F dopants are distributed almost uniformly in both cases. The white boxes in the In/Sn maps indicate the position at which the line profiles in the bottom were obtained. The EDS maps were acquired at 200 keV in an FEI Titan equipped with a Super-X quad EDS detector. c) Typical atomic resolution HAADF-STEM image of a FITO nanocube along the [100] direction showing its BCC crystal structure. The collection angle was selected to be larger than 65 mrad, therefore all atomic columns are corresponding to heavy In atoms, not O atoms. The difference in the contrast at different atomic positions represents the crystal structure of  $\text{In}_2\text{O}_3$  shown schematically in the bottom of panel c). The image was taken at 200 keV in a double Cs corrected FEI Titan Themis. The scale bars are 50 nm in a) and b), and 2 nm in c).

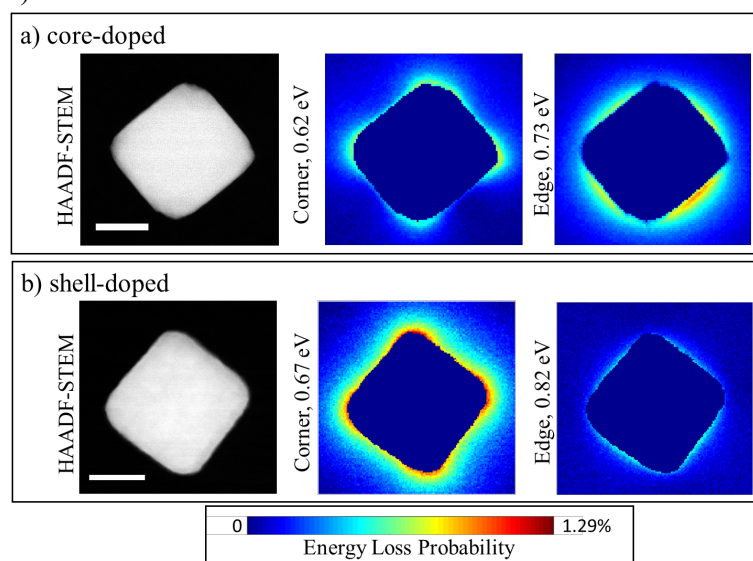


**Fig. 2)** The spatial distribution of electron energy loss corresponding to the corner and edge plasmon modes of individual a) core-doped and b) shell-doped FITO nanocubes, extracted from STEM-EELS spectrum images using the NMF technique. The nanocubes were drop casted on 10 nm thick  $\text{Si}_3\text{N}_4$  TEM grids. The spectrum images were taken at 80 keV in an FEI Titan Themis equipped with a monochromator and a Gatan Quantum ERS spectrometer. (Zero-loss peak FWHM~0.1 eV, Scale bars 50 nm)